Available online at www.sciencedirect.com
SCIENCE DIRECT®
Journal of Power Sources 130 (2004) 163–171
JOURNAL OF POWER SOURCES
www.elsevier.com/locate/jpowsour

Design and experimental tests of control strategies for active hybrid fuel cell/battery power sources

Zhenhua Jiang*, Lijun Gao, Mark J. Blackwelder, Roger A. Dougal

Department of Electrical Engineering, University of South Carolina, Columbia, SC 29208, USA

Received 11 November 2003; accepted 8 December 2003

Abstract

Twenty-first century handheld electronic devices and new generations of electric vehicles or electric airplanes have fueled a need for new high-energy, high-power, small-volume, and lightweight power sources. Current battery technology by itself is insufficient to provide the mandatory long-term power these systems require. Fuel cells are also unable to provide the essentially high peak power demanded by these systems. Hybrid systems composed of fuel cells and secondary batteries could combine the high power density of clean fuel cells and the high energy density of convenient batteries. This paper presents an experimental study on control strategies for active power sharing in such a hybrid fuel cell/battery power source. These control strategies limited the fuel cell current to safe values while also regulating the charging current or voltage of the battery. The several tested control strategies were implemented in MATLAB/Simulink and then tested under the pulsed-current load condition through experiments. Experimental tests were conducted with three control objectives: maximum fuel cell power, maximum fuel cell efficiency, and adaptive.

1. Introduction

Twenty-first century handheld electronic devices and new generations of electric vehicles or electric airplanes have fueled a need for new high-energy, high-power, small-volume, and lightweight power sources for both military and commercial markets [1,2]. Current technology batteries by themselves are insufficient to provide the long-term power (energy between refuelings) that these systems require. Fuel cells of reasonable size may provide the necessary energy, but are then unable to provide the high peak power occasionally demanded by these systems. Hybrid systems composed of fuel cells and secondary batteries combine the high energy density of fuel cells with the high power density of batteries [3,4]. A fuel cell/battery hybrid system could have a number of advantages over each standalone component. Provided that the temperature was not too cold, the battery could enable instant cold-start operation since it can provide a majority of the load power requirement while the fuel cell is warming up. The battery could also condition the power output from the fuel cell to provide a voltage range that is acceptable to the equipment since most devices are already designed to accommodate the source characteristics of a battery. A hybrid system could allow both components to be of smaller dimensions and to operate with higher efficiency since neither would have to provide full load and capacity.

The simplest hybrid configuration results by connecting both the fuel cell and the battery directly to the power bus. This passive hybrid has a number of disadvantages. First, it is necessary to match the nominal voltage of the fuel cell stack to that of the battery, which eliminates much flexibility in the system design. Second, because the power is passively distributed between the fuel cell and the battery, depending on the characteristics of each component, the maximum output current of the hybrid system might be limited by the current capacity of the fuel cell. As an alternative to the passive hybrid, a dc/dc power converter could be placed between the fuel cell and the battery, which would greatly increase the peak output power as shown in Ref. [5] while reducing the system weight and volume. The power sharing between components could then be actively controlled. The purpose of this paper is to present an experimental study on the performance of several control strategies for active power sharing in this hybrid power source.

In the following, the experimental environment and control strategies for active power sharing in the hybrid power source are presented. These control strategies limit the fuel cell current while regulating the charging current or voltage of the battery as necessary. These control strategies were implemented in MATLAB/Simulink and then tested under the pulsed-current load condition through experiments.

* Corresponding author. Tel.: +1-803-777-9314; fax: +1-803-777-8045.
E-mail address: jiang@engr.sc.edu (Z. Jiang).

0378-7753/$ – see front matter © 2003 Elsevier B.V. All rights reserved.
doi:10.1016/j.jpowsour.2003.12.019

Nomenclature

A_{cell}	area of each cell (cm^2)
b, r, m, and n	polynomials determined empirically from experiment data
E_0	standard potential of H_2–O_2 reaction (V)
ΔG_T	change in free energy of the electrochemical oxidation of the fuel (J)
ΔH_0	enthalpy change for the total oxidation reaction of the fuel (J)
I	output current from the fuel cell stack (A)
I_{mpp}	current of the fuel cell corresponding to the maximum power point (A)
N_{cell}	series number of the cells in the fuel cell stack
P_{fc}	output electrical power of the PEM fuel cell stack (W)

Greek symbol

η_{max}	maximum theoretical efficiency of the fuel cell

Experimental tests were conducted with three control objectives: to maximize the power produced by the fuel cell, to maximize the efficiency of the fuel cell, and an adaptive strategy that chooses either maximum power or maximum efficiency depending on state-of-charge of the battery. Experiment results are given and analyzed in this paper.

2. Experimental setup

A hybrid fuel cell/battery power source was built using an H-Power D35 PEM fuel cell stack, a number of Sony US18650 lithium-ion cells, and a dc/dc power converter controlled by a programmable device. Fig. 1 shows the block diagram of the experiment setup and Table 1 describes the main components. The load was connected directly in parallel with the battery while the fuel cell stack was buffered from the load by a synchronous buck converter that was controlled by the system controller. The battery was charged by the fuel cell stack when the load was small and discharged into the load when the load was large. The duty cycle of the power converter was the single control input.

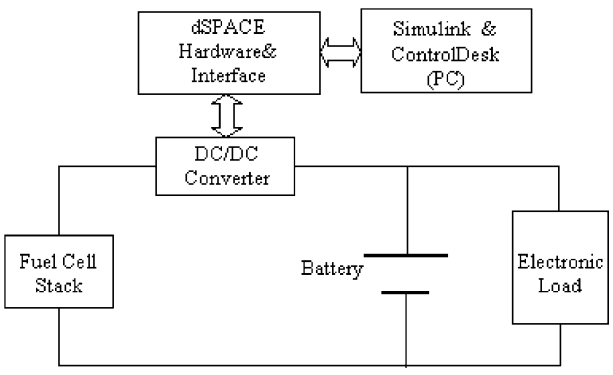

Fig. 1. Block diagram of the experiment setup.

Table 1
Components used in the experiment

Component	Description	Number/comments
PEM fuel cell stack	H-power DS35	25 cells in series
Li-ion battery pack	Sony US18650	3 cells in series; 2 strings in parallel
Load	Chroma 6310	Digitally controllable via GPIB
dc/dc converter	Synchronous buck converter	
Controller	dSPACE DS1103 controller board	

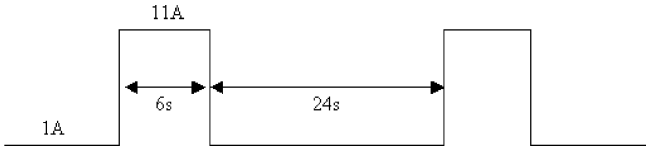

Fig. 2. Profile of the pulse current of the load.

The H-Power D35 PEM fuel cell stack had a nominal power capacity of 35 W and nominal open-circuit voltage of 24 V. Six Sony US18650 lithium-ion cells were used, three cells in series and two such strings in parallel. The nominal capacity of each cell was 1400 mAh. In this configuration, the nominal output voltage of the hybrid power source was 12 V. Fig. 2 shows the current profile of the programmable electronic load. The electronic load accurately drew a pulse current with a period of 30 s. The low current was 1 A for 24 s and the high current was 11 A for 6 s. The average power of the load was about 28 W. This cycle was intentionally chosen for the purpose of investigating the performances of different control strategies, but of course in a practical application, the power of the load might vary more randomly and not so regularly. Fig. 3 schematically shows the circuit diagram of the synchronous buck converter. A voltage chopper consisting of a main switch Q_1 and a secondary switch Q_2 (operating as a synchronous rectifier) converts the voltage from the fuel cell stack to an appropriate lower voltage. The synchronous rectifier was chosen (instead of a junction diode) because the voltage drop of the MOSFET switch as

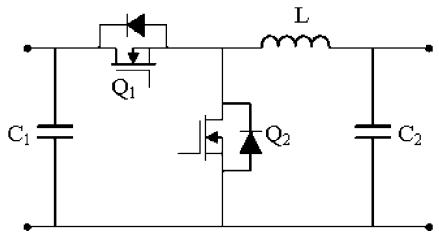

Fig. 3. Diagram of the synchronous buck converter.

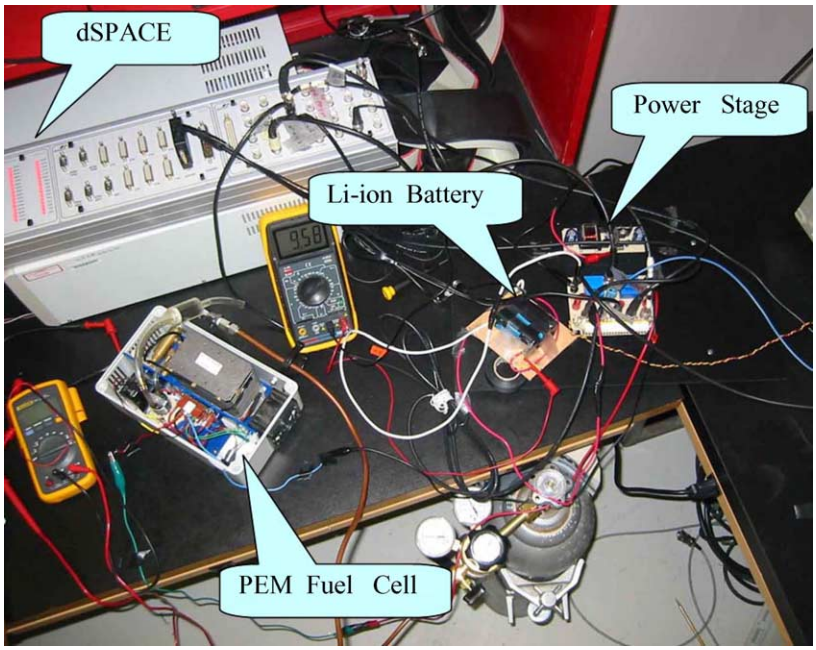

Fig. 4. Photograph of the experiment environment.

synchronous rectifier is about 0.1 V, better than a junction diode (0.6 and 1.0 V) by a factor of 6–10. The lower voltage drop of the synchronous MOSFET translates into higher system efficiency. The power inductor L filters the ripple in the output current. The capacitor C_1 filters the input, while capacitor C_2 smoothes the ripple in the output voltage.

The control code was executed on a general-purpose dSPACE controller board (Model DS1103 PPC). The control algorithm was first developed in MATLAB/Simulink and then compiled and downloaded to the dSPACE controller board. The fuel cell current, battery current, and battery voltage were measured by the dSPACE controller board (via the onboard A/D converters). The reference values of these voltages and currents are identified as I_{rfc}, V_{rb} and I_{rb}, respectively. The real-time controller calculated the duty cycle and provided the switch duty command to the buck converter. The circuit protection functions—limiting the fuel cell current, battery voltage, and battery current—were also implemented within the software. Fig. 4 shows a photograph of the experiment environment.

3. Control strategies for active power sharing

The output electrical power and the overall efficiency are the most important performance indicators. Since the power available from the fuel cell stack is limited, it may sometimes be necessary or desirable for the fuel cell to operate near its maximum power point. The empirical equation (1) approximately describes the electrical output power of a PEM fuel cell stack [6]:

$$P_{fc} = N_{cell} \times \left[E_0 - b\log\left(\frac{I}{A_{cell}}\right) - r\frac{I}{A_{cell}} - m\exp\left(n\frac{I}{A_{cell}}\right)\right] I \quad (1)$$

where P_{fc} is the electrical output power of the PEM fuel cell stack (W), E_0 the standard potential of the H_2–O_2 reaction (V), I the output current from the fuel cell stack (A), N_{cell} the number of cells connected in series, A_{cell} the area of each cell (cm^2), and b, r, m, and n the polynomials determined empirically from experiment data. Obviously the output electrical power P_{fc} reaches the maximum point when $\partial P_{fc}/\partial I = 0$. We will label the current corresponding to maximum power as I_{mpp}.

The efficiency of a fuel cell itself (without considering peripheral components) is maximized at zero delivered power, and has a maximum theoretical value given by

$$\eta_{max} = \frac{\Delta G_T}{\Delta H_0} \quad (2)$$

where ΔG_T is the change in free energy of the electrochemical oxidation of the fuel (J) and ΔH_0 the enthalpy change for the total oxidation reaction of the fuel (J). However, for the entire fuel cell system, which includes parasitic losses for items such as pumps, fans, blowers, heat exchangers, and control electronics, the maximum efficiency point does not occur at zero current, but instead is at some finite current. The practical efficiency of the entire fuel cell power source is quite different from the theoretical value for the cell alone and depends on the system configuration (balance of plant components) and

the operating conditions (e.g. temperature, pressure, and fuel used) as explained more fully in Ref. [7] which developed, defined, and discussed important performance parameters and presented an analytical, three-parameter model that was independent of any specific fuel cell system. According to this model maximum efficiency occurs somewhere below the maximum power point between I_{mpp} and zero.

In our study, three control strategies were tested on the hardware based on the following different objectives.

3.1. Strategy 1: maximum fuel cell power (Test 1)

This strategy aimed to draw maximum electrical power from the fuel cell stack, which occurred at approximately 2 A. For the purposes of the work reported here, it was not our objective to identify this maximum power point, but rather to show that the plant could be operated at that point once it was identified. We simply set the reference current from the fuel cell stack at the 2 A value. The reference charging current of the battery was also set to 2 A, according to the maximum safe charging rate of the batteries.

3.2. Strategy 2: maximum fuel cell efficiency (Test 2)

This strategy aimed to achieve maximum overall efficiency of the fuel cell system, which was empirically observed to occur near 1.25 A. Thus, the reference current of the fuel cell was set at 1.25 A. Again, for the purposes of the work reported here, it was not our objective to identify this maximum efficiency point, but rather to show that the plant could be operated at that point once it was identified. The reference charging current of the battery was again set at 2 A.

3.3. Strategy 3: adaptive strategy (Test 3)

If the average power demand of the load was larger than the power delivered at the maximum efficiency point, but less than full rated power of the fuel cell power source, then eventually the battery would become fully charged if Strategy 1 was followed or fully depleted if Strategy 2 was followed. The adaptive strategy aimed to maintain a relatively constant battery voltage by switching between Strategies 1 and 2. When the battery voltage dropped below a preset

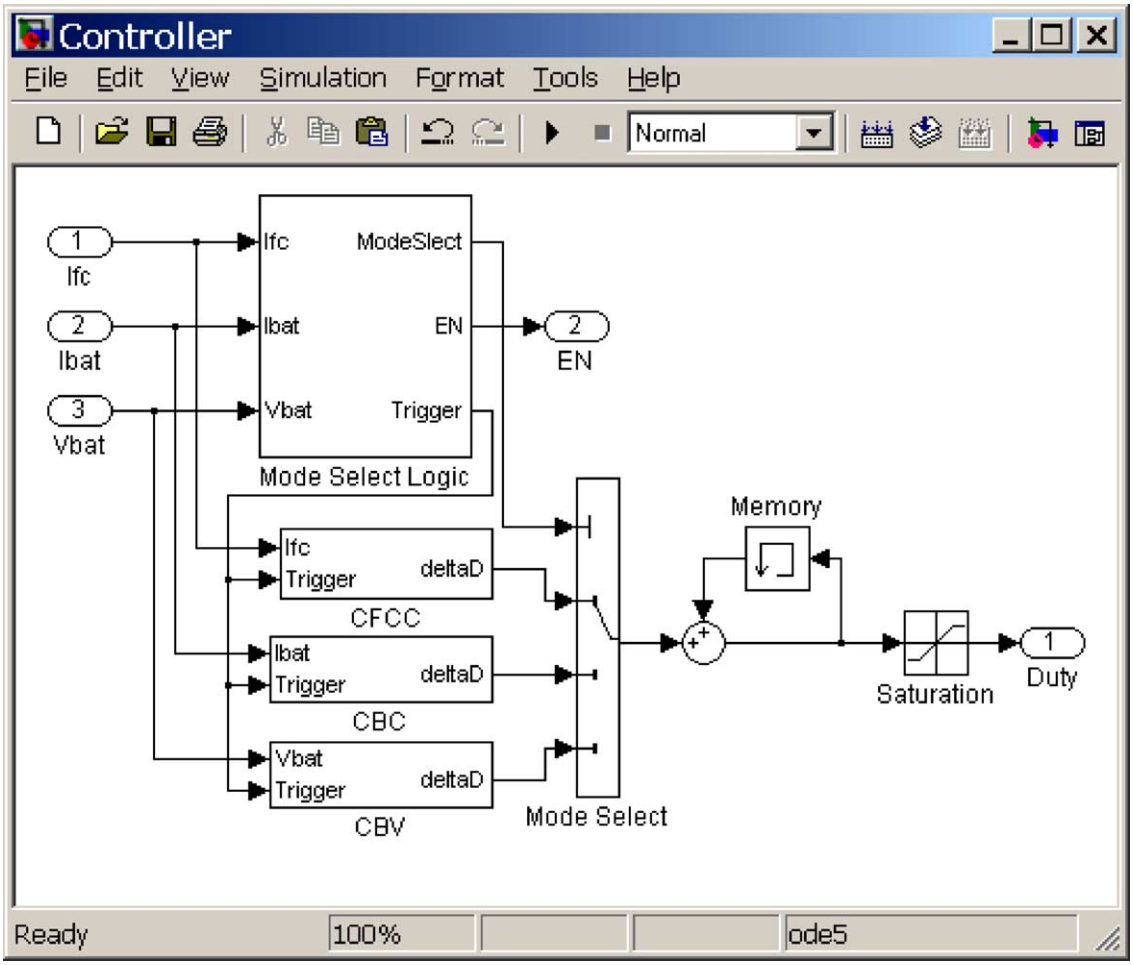

Fig. 5. Simulink implementation of control strategy.

value, the maximum power strategy was applied and when it exceeded another preset value, the maximum efficiency strategy was applied.

Each of these control strategies must limit the fuel cell current while regulating either the charging current or the voltage of the battery as appropriate at the particular state-of-charge of the battery. Only the duty cycle of the power converter can be controlled. By changing the duty cycle, the output current of the fuel cell, or the voltage or current of the battery can be regulated. Thus there are three regulation modes: fuel cell current limit (FCCL) mode, battery current limit (BCL) mode, and battery voltage limit (BVL) mode, each based on different goals. In the hybrid power source, the battery voltage is an important index of the regulation mode. If the battery voltage exceeds the high limit voltage, which may correspond to the condition of no load or light load as well as high battery charge, then battery voltage limit mode must apply to prevent overcharging the battery. Under this mode, the output current of the fuel cell and the charging current of the battery should be below the rated currents. If the battery voltage is below the high limit voltage, which may correspond to the condition of heavy load or light load coupled with low battery charge, then either fuel cell current limit mode or battery current limit mode may apply, depending on the load. If the current demand is lower than the rated output current of the fuel cell, the charging current of the battery may need to be regulated in order to protect the battery, i.e. battery current limit mode applies. In this case, the fuel cell current is unregulated but is always below the rated current. If the current demand is very high, fuel cell current limit mode applies. In this case, the battery may be discharged or charged at a lower rate but the fuel cell is protected from over-current. For example, when the power source is first turned on, it works under fuel cell current limit mode. If there is no load or a light load, the charging current of the battery may rapidly increase from zero to the limiting value. Then the battery current limit mode must apply to protect the battery. When the battery voltage reaches its upper limit, the battery voltage limit mode applies. Under either BCL mode or BVL mode, if the load increases quickly (i.e. when the fuel cell current reaches its limit), fuel cell current limit mode will apply. Under any of these three modes, the load will be disconnected if the battery discharging current exceeds the safe operating limit.

Each control strategy was implemented in MATLAB/Simulink and then tested under the pulsed-current load condition through simulation and experiments. Experimental validation was performed by compiling the Simulink code of the control algorithm and downloading it to the dSPACE platform to control the real hardware. The Simulink model of the controller is shown in Fig. 5. The main functional blocks in this Simulink model are the mode-select logic module, the current regulation module and the voltage regulation module. The regulation mode was determined by the control strategy explained previously. The current and voltage regulation modules were used to compute the duty cycles to the buck converters according to the reference currents and the reference voltages, respectively. The proportional–integral approach was used to regulate the currents and voltages.

4. Experiment results and discussion

Tests of the three control strategies were conducted on the experiment platform described previously and results are shown in Figs. 6–17 which are described next.

Figs. 6 and 7 show the currents and voltages of the fuel cell and the battery, respectively, under the maximum fuel cell power strategy (Test 1). Finer details of these currents and voltages are shown in Figs. 8 and 9, respectively. From Fig. 8, it can be seen that when the load drew low power the fuel cell stack provided about 1.6 A current, supplying 1 A current to the load and simultaneously charging the battery

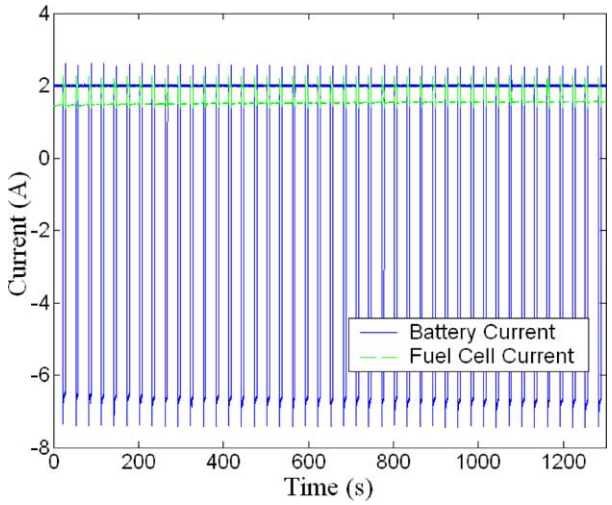

Fig. 6. Current waveforms of the fuel cell and battery in Test 1.

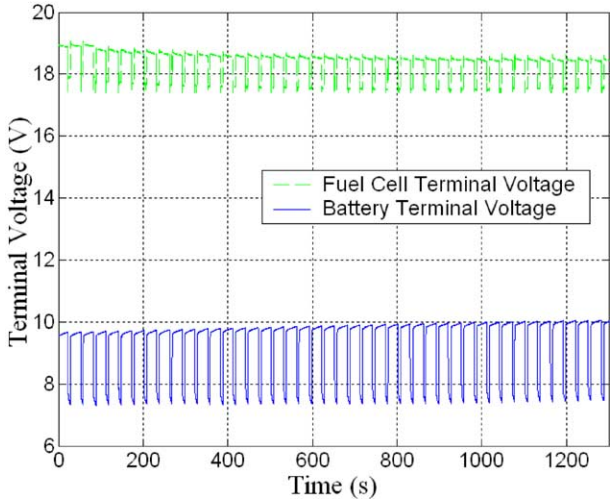

Fig. 7. Voltage waveforms of the fuel cell and battery in Test 1 (top: fuel cell voltage; bottom: battery voltage). Over cycles, the battery voltage increased and the fuel cell voltage decreased.

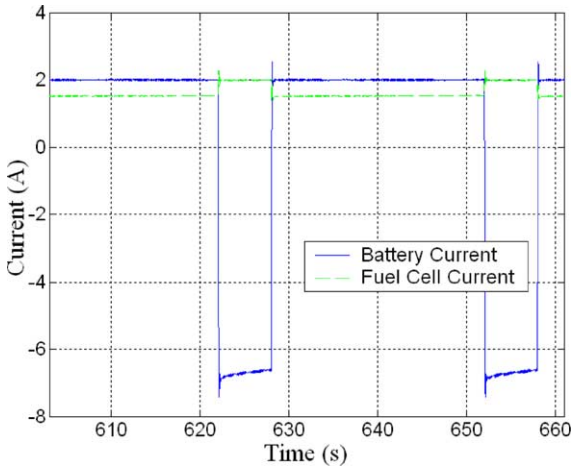

Fig. 8. Detail of current waveforms of the fuel cell and battery in Test 1. When the load drew low power, the fuel cell output about 1.6 A current, supplying 1 A current to the load and charging the battery at 2 A current. When the load drew peak power, the fuel cell produced 2 A current and the battery discharged at around 7 A current.

at 2 A. (The currents do not sum to zero because the voltages are different at the input and output of the power converter.) It is shown in Fig. 9 that the battery voltage gradually increased during the low-power period. During this time, the charging current of the battery was regulated (BCL mode applied), and the fuel cell current was less than the reference value and depended on the load demand. When the load power increased, the fuel cell supplied 2 A current (corresponding to its maximum power point). At this time, the battery discharged at around 7 A, and the voltage dropped suddenly and then gradually decreased further. During this time, the fuel cell current was regulated (FCCL mode applied) and the discharging current of the battery depended on the load. It is seen that the regulation mode was correctly selected. It is worthwhile to note that if the load had drawn a much lower peak current (for example, 3 A), the battery would have been charged at a lower current while the fuel cell would have supplied 2 A current. Fig. 6 shows that the currents of the fuel cell and the battery varied periodically since they were regulated alternately. From Fig. 7, it can be seen that after three cycles the fuel cell voltage suddenly dropped. This was because the fan of the fuel cell stack started when the temperature of the stack reached the thermostat threshold and some amount of power from the fuel cell was diverted to drive the fan. An important observation from Fig. 7 is that over many cycles the battery voltage increased. This was due to the fact that the average power demand of the load was less than the maximum output power of the fuel cell stack. During any one cycle, the net power transferred to the battery was positive, which caused the battery voltage to increase slightly by the end of each cycle. If the load had drawn more average power than the maximum power available from the fuel cell stack, the battery voltage would have decreased and the battery would have run down finally to depletion. Fig. 7 also shows that over many cycles the fuel cell voltage decreased. This was because the fuel cell needed to provide more power to charge the battery as the battery voltage increased (since the charging current was constant, as the battery voltage increased, so did the charging power).

Figs. 10 and 11 show the currents and voltages of the fuel cell and the battery, respectively, under the maximum fuel cell efficiency strategy (Test 2). Details of these currents and voltages are shown in Figs. 12 and 13, respectively. From Fig. 12, one can see that the fuel cell stack provided 1.25 A current (corresponding to its maximum efficiency point) at all times. When the load drew low power the battery was charged at about 1.5 A current (less than the battery current limit) because the fuel cell did not provide enough electrical power to charge the battery at maximum rate and power the load. The battery voltage increased a little bit during the low-power period as shown in Fig. 13. When the load drew

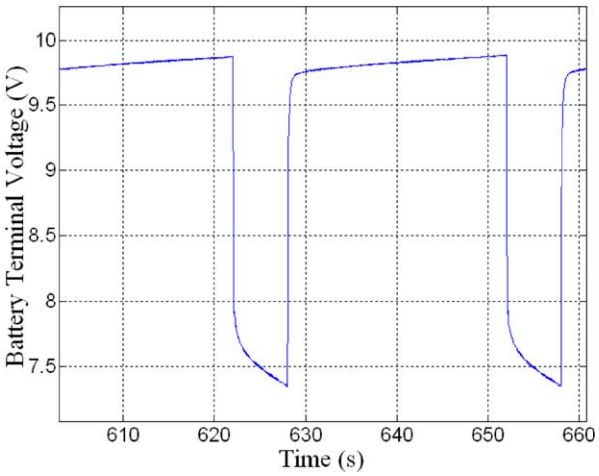

Fig. 9. Detail of the battery terminal voltage in Test 1. The voltage of the battery increased when it was charged and decreased when it was discharged.

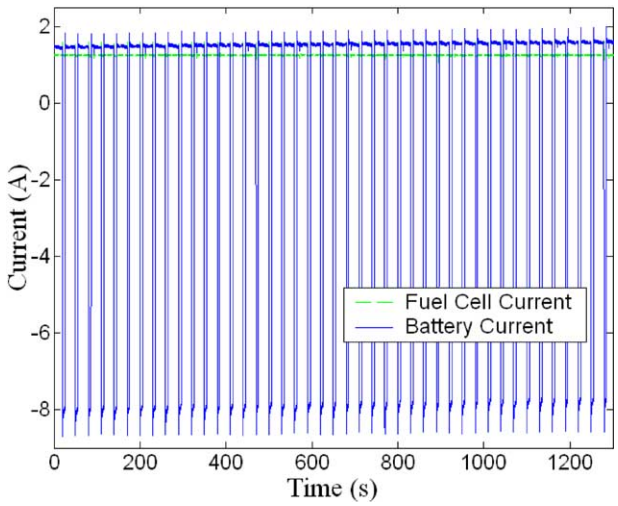

Fig. 10. Current waveforms of the fuel cell and battery in Test 2.

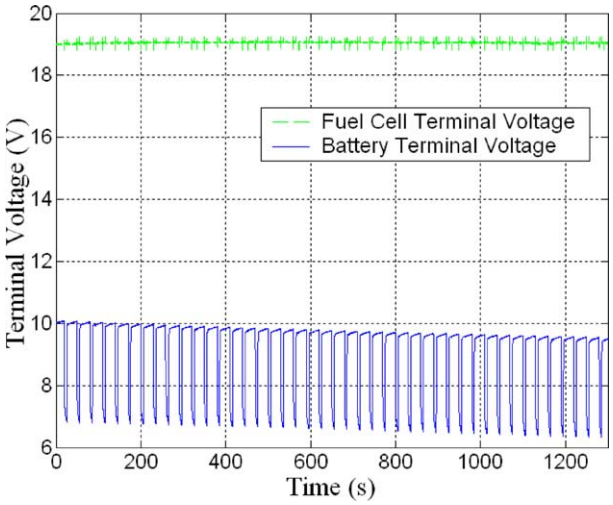

Fig. 11. Voltage waveforms of the fuel cell and battery in Test 2 (top: fuel cell voltage; bottom: battery voltage). Over cycles, the battery voltage decreased and the fuel cell voltage maintained at a constant level.

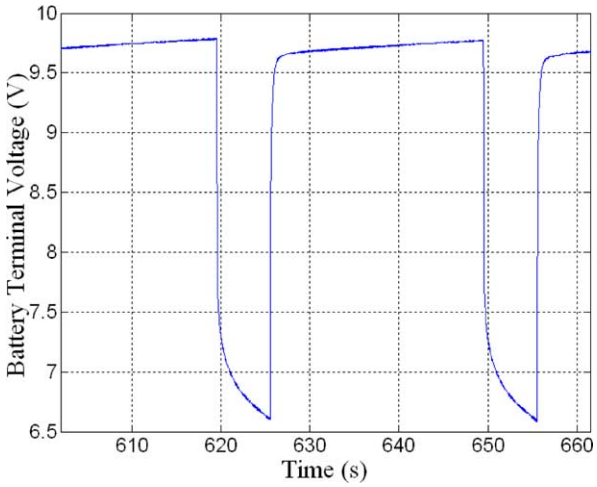

Fig. 13. Detail of the battery terminal voltage in Test 2. The voltage of the battery increased when it was charged and decreased when it was discharged.

a larger power, the battery discharged at around 8 A and the voltage decreased. The discharge current of the battery was a little higher than that in Test 1 because the fuel cell was supplying less total power in Test 2 when operating at the maximum efficiency point. From Fig. 13, it is seen that over many cycles the battery voltage decreased. This was because the average power of the load was higher than the output power of the fuel cell stack. During any one cycle, the net power transferred to the battery was negative. If the load had drawn less average power than the power available from the fuel cell stack at the maximum efficiency point, the battery voltage would have increased. We can also see that over many cycles the fuel cell voltage maintained a constant level because the fuel cell current was constant. It is interesting to note that in this test the fan of the fuel cell stack did not start. This resulted from the fact that with the maximum efficiency strategy the fuel cell produced less heat and the temperature of the stack did not reach the mandatory cooling threshold. This point is really significant to the users from the economic viewpoint. First, the stack itself used less hydrogen, and second, the fan stopped drawing power from the fuel cell stack. So there was a double benefit to operate in this mode. The savings of hydrogen were probably larger than a simple estimate would yield.

Differences in the change of the battery terminal voltages in Tests 1 and 2 can be clearly seen in Fig. 14. Over many cycles, the battery voltage increased gradually under maximum power strategy but decreased gradually under maximum efficiency strategy. It is shown that after 20 min of operation, the battery voltage with Strategy 1 was about 1 V higher than that with Strategy 2. With maximum power strategy, the battery would finally become charged to the full

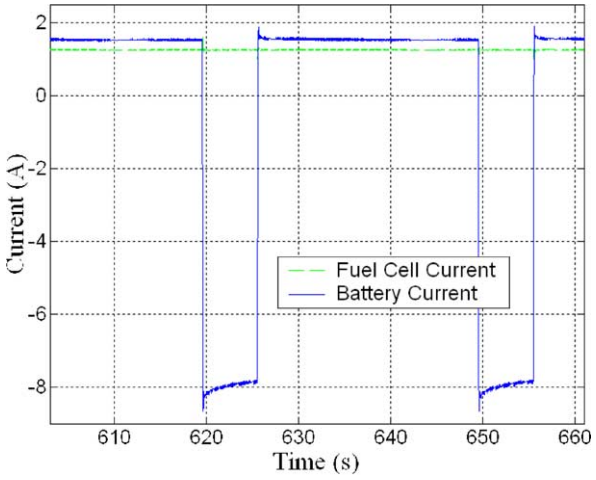

Fig. 12. Detail of current waveforms of the fuel cell and battery in Test 2. The fuel cell stack provided 1.25 A current all the time. When the load drew low power, the battery was charged at 1.5 A current. When the load drew peak power, the battery discharged at approximately 8 A current.

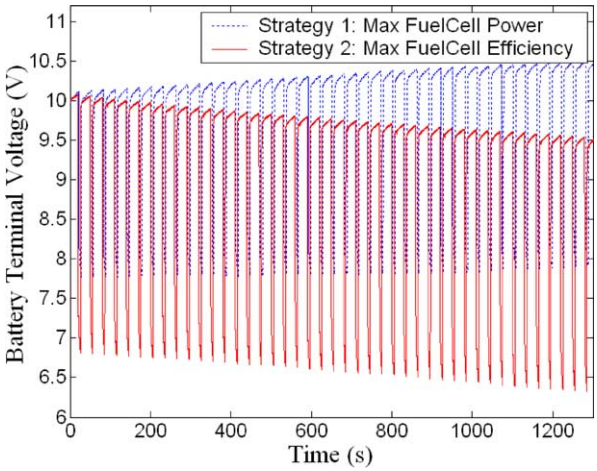

Fig. 14. Comparison of the battery terminal voltages in Tests 1 and 2. Over many cycles, the battery voltage increased under maximum power strategy but decreased under maximum efficiency strategy.

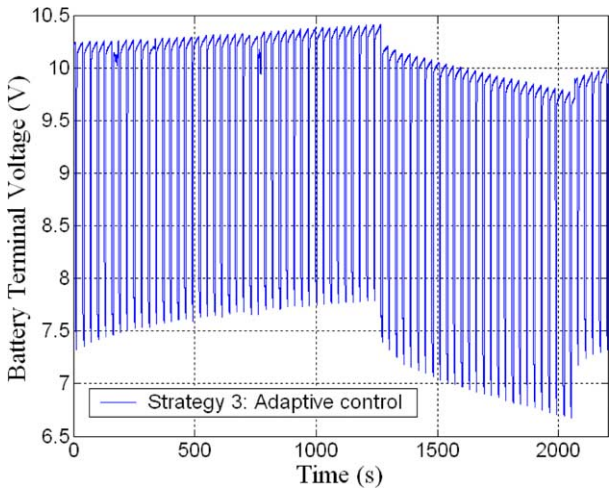

Fig. 15. Battery terminal voltage in Test 3. When the battery was charged to a certain level under maximum power strategy, the maximum efficiency strategy applied. When the battery was run down to a preset level under maximum efficiency strategy, the maximum power strategy was applied.

state but the efficiency would not be maximized. With maximum efficiency strategy, the fuel cell would achieve maximum efficiency but the battery would run down finally to depletion. However, the advantages of both strategies could be utilized reasonably in the adaptive strategy (see Fig. 15). When the battery was charged to a certain level under the maximum power strategy, the maximum efficiency strategy applied. When the battery is run down to a preset level under maximum efficiency strategy, the maximum power strategy applied. The battery voltage varied within a smaller range for this strategy. The fuel cell current in Test 3 is shown in Fig. 16 and the detail is shown in Fig. 17. When the strategy was switched, the current limit of the fuel cell changed.

An obvious extension of this strategy would regulate the fuel cell current on a continuous basis. Instead of cycling between the high-power and high-efficiency modes, the current setpoint would be controlled continuously based on

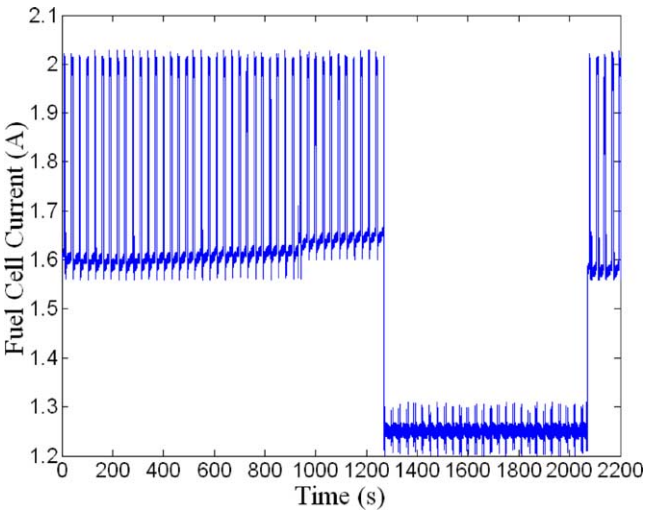

Fig. 16. Waveform of the fuel cell current in Test 3.

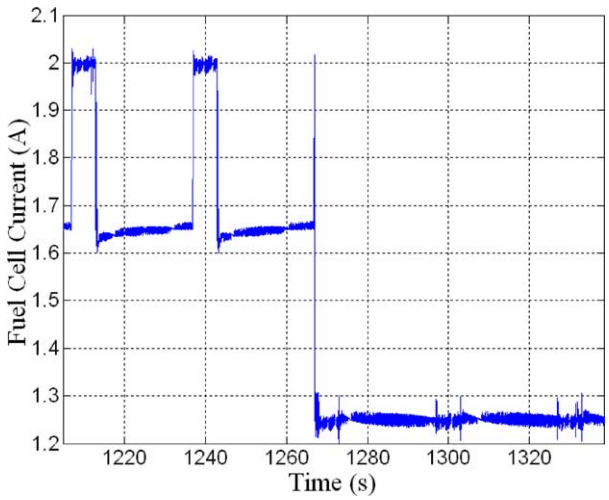

Fig. 17. Detail of the fuel cell current in Test 3. The fuel cell current changed to a smaller value when the maximum efficiency strategy was applied.

the battery voltage (or state-of-charge). For instance, when the battery is 80% full, the setpoint would be closer to the high-efficiency setpoint, but at 40% state-of-charge the setpoint would be closer to the maximum-power setpoint.

5. Conclusion

The topology of an active fuel cell/battery hybrid was presented and control strategies for active power sharing in this hybrid power source were described. In this configuration (fuel cell-regulated, battery-floating) these control strategies limit the fuel cell current while regulating the charging current or voltage of the battery as necessary. These control strategies were implemented in MATLAB/Simulink and then experimentally tested under a pulse-current load condition.

Tests of three control objectives were conducted. With maximum power strategy, the fuel cell can output as much power as possible. With maximum efficiency strategy, the fuel cell can run at as high efficiency as possible. Over many power cycles, the battery voltage increased under the maximum power strategy but decreased under the maximum efficiency strategy. With the former strategy, the battery would be finally charged to the full state but the efficiency would not be maximized. With the latter strategy, the fuel cell would achieve maximum efficiency but the battery would finally run down to depletion. However, the advantages of both strategies could be utilized reasonably in the adaptive strategy. When the battery was charged to a certain level under the maximum power strategy, the maximum efficiency strategy applied. When the battery was run down to a preset level under maximum efficiency strategy, the maximum power strategy was applied. The adaptive strategy of cycling between high-power and high-efficiency modes could maintain the battery voltage at an appropriate level and achieved good output power and good efficiency of the fuel cell stack.

Acknowledgements

This work was supported under agreement DAAB07-03-3-K416 with the US Army Communications-Electronics Command (CECOM) for Hybrid Advanced Power Sources with guidance from the RDECOM/CERDEC Fuel Cell Technology Team at Fort Belvoir, VA, and by the US Office of Naval Research under contract N000140310952.

References

[1] T.B. Atwater, P.J. Cygan, F.C. Leung, Man portable power needs of the 21st century. I. Applications for the dismounted soldier. II. Enhanced capabilities through the use of hybrid power sources, J. Power Sour. 91 (1) (2000) 27–36.
[2] R.F. Nelson, Power requirements for batteries in hybrid electric vehicles, J. Power Sour. 91 (1) (2000) 2–26.
[3] P.B. Jones, J.B. Lakeman, G.O. Mepsted, J.M. Moore, A hybrid power source for pulse power applications, J. Power Sour. 80 (1/2) (1999) 242–247.
[4] C.E. Holland, J.W. Weidner, R.A. Dougal, R.E. White, Experimental characterization of hybrid power systems under pulse current loads, J. Power Sour. 109 (1) (2002) 32–37.
[5] L. Gao, Z. Jiang, R. Dougal, An actively controlled fuel cell/battery hybrid to meet pulsed power demands, J. Power Sour., in press.
[6] J. Kim, S.M. Lee, S. Srinivasan, Modeling of proton exchange membrane fuel cell performance with an empirical equation, J. Electrochem. Soc. 142 (8) (1995) 1670–2674.
[7] B. Thorstensen, A parametric study of fuel cell system efficiency under full and part load operation, J. Power Sour. 92 (1/2) (2001) 9–16.